Magnetic field and temperature tuning of resonant Raman scattering in diluted magnetic semiconductors

D. L. Peterson, D. U. Bartholomew, A. K. Ramdas, and S. Rodriguez
Department of Physics, Purdue University, West Lafayette, Indiana 47907
(Received 13 December 1984)

We report the observation of the resonance enhancement of the Raman line in $Cd_{1-x}Mn_xTe$ associated with the LO phonons in combination with the spin flip of Mn^{2+}. The resonance condition is fulfilled when the large magnetic-field-induced exciton splitting allows one of its components to be brought into coincidence with the Raman line. The exciton splittings are due to the large effective g factors of the conduction and valence bands arising from the strong Mn^{2+}—band-electron exchange interaction. The associated temperature tuning is also observed at a constant magnetic field. The feasibility of magnetic field tuning of resonance conditions for Raman scattering in diluted magnetic semiconductors is a result of the sensitive manner in which excitonic splittings depend on magnetic field, temperature, and concentration of magnetic ions. In addition, new higher order spin-flip Raman scattering is observed; an interpretation for their occurrence is presented.

I. INTRODUCTION

The substitution of a magnetic ion—typically manganese—for the group II host atom in a II-VI semiconductor results in a class of semiconductors known as diluted magnetic semiconductors (DMS). Thanks to the strong exchange coupling between the $3d$ electrons of Mn^{2+} and the band electrons, these semiconductors exhibit novel semiconducting and magnetic properties.[1,2] The free exciton in $Cd_{1-x}Mn_xTe$, for example, undergoes a large Zeeman splitting[3] even in moderate magnetic fields and underlies the observed very large Faraday rotation.[4] These effects can be described in terms of an effective g factor for the band electrons that is two orders of magnitude larger than that for CdTe. This g factor is a strong function of the applied magnetic field H, temperature T, and manganese mole concentration x, showing a characteristic saturation at large H/T. In contrast, the $3d$ electrons of Mn^{2+} exhibit $g\cong 2$ as has been deduced from the Raman—electron-paramagnetic-resonance (Raman-EPR:ω_{PM}) experiments.[5,6] Even in these experiments the authors noted that the Raman-EPR signals show a dramatic increase when the exciting laser energy $\hbar\omega_L$ approaches interband transition energies E_g; a microscopic picture involving virtual interband transitions between the valence-band maximum and the conduction-band minimum accompanied by a spin flip of Mn^{2+} through exchange interaction has been invoked to explain the effect. Being a polar crystal, the Raman EPR can also appear in conjunction with the exciton of LO phonons, i.e., Raman lines appear with frequency shifts $\omega_{LO}\pm\omega_{PM}$.[5,6]

The focus of the present paper is a striking and novel manifestation of resonance enhancement of the $\omega_{LO}\pm\omega_{PM}$ Raman lines when the energy of the scattered radiation equals that of a Zeeman component of the exciton, the resonance condition being produced by magnetic field or temperature tuning.

II. EXPERIMENTAL RESULTS AND INTERPRETATION

The phenomena described in this paper—the Raman and photoluminescence spectra—were recorded with a variable temperature optical magnet cryostat, a Kr^+ laser, and a computer controlled grating spectrometer and associated photon counting electronics.[6,7] The scattering geometries are described in Ref. 6; in the following, $\hat{\mathbf{k}}_s$ denotes the direction of the scattered radiation whereas $\hat{\boldsymbol{\sigma}}_\pm=(\hat{\mathbf{x}}\pm i\hat{\mathbf{y}})/\sqrt{2}$, the circular polarizations of positive and negative helicities, and $\hat{\mathbf{z}}$ the direction of $\mathbf{H}$, the applied magnetic field. The results reported in this paper were obtained in the right-angle scattering geometry with the magnetic field $\mathbf{H}\|\hat{\mathbf{k}}_s$. The scattered light was analyzed with a quarter-wave plate as either $\hat{\boldsymbol{\sigma}}_+$ or $\hat{\boldsymbol{\sigma}}_-$, allowing the $(\hat{\mathbf{z}},\hat{\boldsymbol{\sigma}}_\pm)$ polarization configurations in some of the experiments and are specified in the figure captions.

Figure 1 shows the Raman spectrum of $Cd_{0.95}Mn_{0.05}Te$ in the right-angle scattering geometry excited with the 7525-Å line in an external magnetic field, $H=60$ kG, and at a temperature $T=5$ K. The exciting radiation is near resonance with the free exciton transitions. The sharp, magnetic-field-induced Raman line labeled PM, attributed to the spin flip of the $3d$ electrons of the Mn^{2+} ions, has been studied in detail by us in DMS, in particular $Cd_{1-x}Mn_xTe$.[6] In the paramagnetic phase, the application of an external magnetic field lifts the sixfold degeneracy of the $^6S_{5/2}$ ground state of the Mn^{2+} ion. (The crystal-field splitting, too small to be observed in Raman scattering, is ignored here.) The Zeeman multiplet of the ground state of Mn^{2+} is thus characterized by $E(m_S)=g\mu_B Hm_S$, where $g=2$, $\mu_B=$ the Bohr magneton and m_S, the spin projection along $\mathbf{H}$. The PM line originates from the $\Delta m_S=+1$ spin-flip transitions between adjacent sublevels of the Zeeman multiplet yielding a Raman shift of $\hbar\omega_{PM}=g\mu_B H$. The Stokes line is observed in either the $(\hat{\boldsymbol{\sigma}}_+,\hat{\mathbf{z}})$ or $(\hat{\mathbf{z}},\hat{\boldsymbol{\sigma}}_-)$ polarization config-

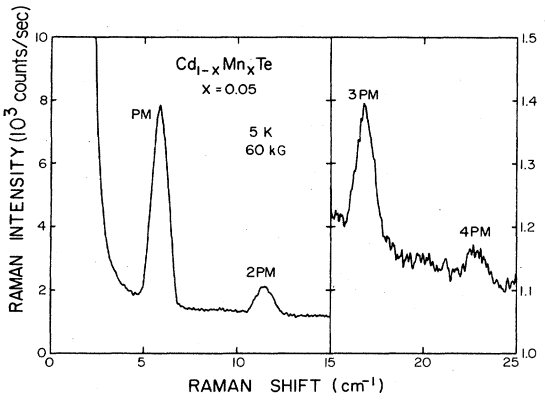

FIG. 1. Stokes Raman lines at $n\omega_{PM}$ ($n=1,2,3,4$) resulting from $\Delta m_S=+n$ spin-flip transitions in the Zeeman multiplet of the ground state of the $3d$ shell of Mn^{2+} in $Cd_{0.95}Mn_{0.05}Te$. Exciting wavelength $\lambda_L=7525$ Å, power $P_L=90$ mW; applied magnetic field $H=60$ kG and temperature $T=5$ K. The spectrum for shifts greater than 15 cm^{-1} is the average of ten scans. Right-angle scattering geometry was used and scattered light, propagating parallel to the magnetic field, was not analyzed.

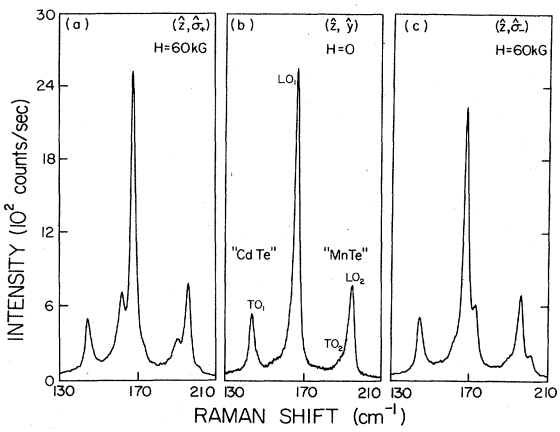

FIG. 2. Raman spectra of $Cd_{1-x}Mn_xTe$, $x=0.10$, showing Raman lines with shifts of $\omega_{LO_1}\pm\omega_{PM}$ and $\omega_{LO_2}\pm\omega_{PM}$, where LO_1 and LO_2, respectively, are the "CdTe-like" and "MnTe-like" LO phonons. Incident light along $\hat{\mathbf{k}}_i||[\bar{1}10]$, polarized along $[1\bar{1}0]||\mathbf{H}||\hat{\mathbf{k}}_S$, the scattering direction. Scattered light analyzed for $\hat{\boldsymbol{\sigma}}_+$ in (a) and $\hat{\boldsymbol{\sigma}}_-$ in (c) and along [001] in (b). $T=120$ K, H=60 kG, and $\lambda_L=7525$ Å.

urations, while the anti-Stokes component appears in $(\hat{\boldsymbol{\sigma}}_-,\hat{\mathbf{z}})$ or $(\hat{\mathbf{z}},\hat{\boldsymbol{\sigma}}_+)$. Under conditions when the laser photon energy approaches that of the band gap, we observed Raman features which can be attributed to the $\Delta m_S=\pm2$ spin-flip transitions as well as combinations of the $\Delta m_S=\pm1$ transitions with the LO phonons.[8] The Stokes component of the Raman line at $2\omega_{PM}$ is observed in $(\hat{\boldsymbol{\sigma}}_+,\hat{\boldsymbol{\sigma}}_-)$ whereas the anti-Stokes occurs in $(\hat{\boldsymbol{\sigma}}_-,\hat{\boldsymbol{\sigma}}_+)$, both in the forward scattering geometry.[6] The combination of the spin-flip transition with either of the two LO phonons[6,8] in $Cd_{1-x}Mn_xTe$ occurs with shifts $\omega_{LO}\pm\omega_{PM}$ in the $(\hat{\boldsymbol{\sigma}}_\pm,\hat{\mathbf{z}})$ or $(\hat{\mathbf{z}},\hat{\boldsymbol{\sigma}}_\mp)$ configurations. In Fig. 2 the Raman spectrum of $Cd_{0.9}Mn_{0.1}$ Te showing the $\omega_{LO}\pm\omega_{PM}$ lines is reproduced from our results reported in Ref. 6. Since these lines appear only under band-gap resonance and involve only the LO phonons and, hence, the Fröhlich interaction, an interband, or equivalently an excitonic, Raman mechanism was proposed.[6] This mechanism provides an explanation for the polarization and resonance characteristics of the Raman transitions. The scattering amplitude for this Raman mechanism is proportional to the magnitude of the exchange coupling between the Mn^{2+} ions and the band electrons which is especially strong in these alloys. Adapting Loudon's theory for optical phonons,[9] the scattering cross section for such a three-step process can be written as being proportional to

$$\left|\frac{\langle n_S+1,0\,|\,H_{eR}\,|\,n_S,b\rangle\langle m_S+1,b\,|\,H_{ex}\,|\,m_S,a\rangle\langle n_L-1,a\,|\,H_{eR}\,|\,n_L,0\rangle}{(\omega_b+\omega_{PM}-\omega_L)(\omega_a-\omega_L)}+\cdots\right|^2, \tag{1}$$

where the ellipsis represents five additional terms. Here H_{eR} is the electron-photon interaction Hamiltonian, H_{ex} is the exchange Hamiltonian describing the exchange interaction between $3d$-localized states of Mn^{2+} and conduction (valence) electrons, n_L,n_S are the occupation numbers of the incident and scattered photon modes, respectively, and $\hbar\omega_a,\hbar\omega_b$ are the intermediate excitation energies of the virtual electron-hole pair. The other five terms in Eq. (1) are the remaining permutations of the three steps of the Raman process. It is clear that the first term will dominate when $\omega_a\sim\omega_L$ or $\omega_b\sim(\omega_L-\omega_{PM})=\omega_S$, producing a double peak in the frequency dependence of the cross section. The condition of "in resonance" results from the matching of the incident photon energy with that of an electronic excitation whereas "out resonance" occurs when the scattered photon energy equals the energy of such a transition.[10]

In Eq. (1) above, $\hbar\omega_a$ and $\hbar\omega_b$ are the energies of excitation of two states of the exciton with angular momenta differing by one unit. For example, following Twardowski *et al.*,[3] for a $(\hat{\mathbf{z}},\hat{\boldsymbol{\sigma}}_+)$ Stokes line

$$\begin{aligned}\hbar\omega_a&=E_x-3A+B\ ,\\ \hbar\omega_b&=E_x-3A+3B\ ,\end{aligned} \tag{2}$$

where E_x is the exciton energy and

$$\begin{aligned}A&=\tfrac{1}{6}xN_0\alpha\langle S_z^{Mn}\rangle\ ,\\ B&=\tfrac{1}{6}xN_0\beta\langle S_z^{Mn}\rangle\ .\end{aligned} \tag{3}$$

In Eq. (2), it is assumed that the electron-hole exchange and correlation energy is insensitive to H. In Eq. (3), N_0 is the reciprocal of the volume of the primitive cell; $\alpha(\beta)$ is the exchange integral of the $3d$ states of Mn^{2+} and conduction (valence) electrons and $\langle S_z^{Mn} \rangle$ is the average value of the component of Mn^{2+} spin along **H** given by $(\frac{5}{2})B_{5/2}(g\mu_B H/k_B T)$ in the paramagnetic phase. Thus the energies $\hbar\omega_{a,b}$ are characterized by an effective g factor which is a nonlinear function of (H/T).

In Figs. 3(a) and 3(b), we show the photoluminescence spectrum of $Cd_{1-x}Mn_xTe$, $x=0.05$, at 5 K in the absence of a magnetic field. The feature labeled X is attributed to free-exciton recombination[11] and has an energy of $E_x=1.665$ eV, an increase of 70 meV from the value in CdTe.[12] We emphasize that the energy of line X includes the additional binding energy due to the mutual spin polarization of the carriers and of the Mn^{2+} within the exciton orbit, the so-called "bound magnetic polaron" effect. For $x=0.05$, this effect is small as shown in Fig. 2 of Golnik *et al.*[11] and should be unimportant even at a relatively small magnetic field. The energy of this exciton varies linearly with Mn^{2+} concentration[13] in $Cd_{1-x}Mn_xTe$ and the value measured here is in good agreement with that expected. The feature labeled A^0X is attributed to the exciton bound to a neutral acceptor[11] with a binding energy of 9 meV. The feature at 1.608 eV, when corrected for the change in the energy gap, corresponds to the 1.54-eV feature in CdTe which may result from free-electron—to—acceptor transitions;[14] the features at 1.587 and 1.566 eV are the LO phonon replicas of this transition. Similarly, the series of luminescence peaks beginning at $\sim$1.5 eV are the LO phonon replicas of the

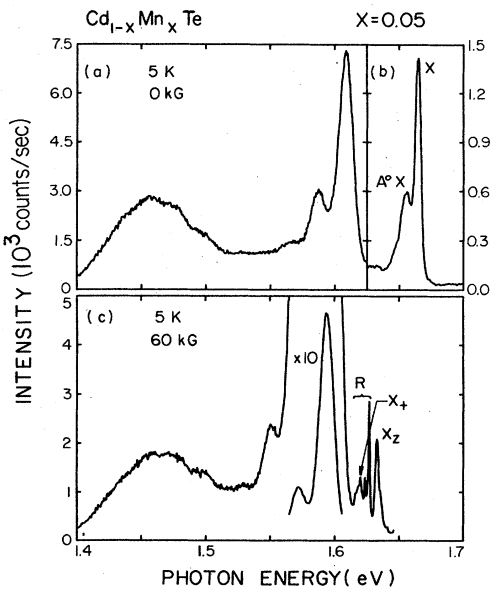

FIG. 3. Photoluminescence spectra of $Cd_{0.95}Mn_{0.05}Te$ at $T=5$ K with $H=0$ for (a) and (b), $H=60$ kG for (c), $\lambda_L=7525$ Å for (a) and (c), $\lambda_L=6764$ Å for (b), and $P_L=25$ mW for all cases. Raman features are denoted by R. In (c), the features between 1.55 and 1.6 eV are also displayed on a scale reduced by 10.

transitions associated with a vacancy-donor complex $(V_{Cd}^{2-}D^+)$,[15] where the donors in this case are presumed to be interstitial copper atoms[16] introduced during crystal growth. As the magnetic field is increased the free exciton peak increases in intensity and shifts to lower energy sweeping across the A^0X feature.[11] At sufficiently high magnetic fields a splitting in the free exciton feature is observed.[17] Two of these are present in Fig. 3(c); the low-energy component labeled X_+ appears in the $\hat{\sigma}_+$ polarization, while the other, X_z, is polarized along $\hat{z}$. The feature associated with the free electron to acceptor transition and its LO phonon replicas shift by 14 meV in a magnetic field of 60 kG.

On the basis of the luminescence spectra, appropriate choices of laser wavelength, sample temperature and magnetic field can be made to achieve conditions of in resonance or out resonance, which can selectively enhance specific features in the Raman spectrum. In the geometry employed in the experiments reported in this paper, the $\omega_{LO}-\omega_{PM}$ line, i.e., the Raman shift with the creation of an LO phonon and the de-excitation of the Mn^{2+} by $\Delta m_S=-1$ involves a virtual transition at an energy $\hbar\omega_a$ for the incident radiation polarized along $\hat{z}$ and another at $\hbar\omega_b$ for scattered radiation having $\hat{\sigma}_+$ polarization. With 7525-Å ($\hbar\omega_L=1.648$ eV) laser line, the in resonance condition is nearly fulfilled; with A and B in Eq. (3) for $x=0.05$, $T=5$ K, and $H=60$ kG, we estimate the energies of X_z and X_+, the components which move to lower energies with increasing H, to be 1.636 and 1.603 eV, respectively.[18] Thus, it is clear that the in-resonance condition is satisfied even more closely whereas the out resonance for $\omega_{LO}-\omega_{PM}$ can now be realized. The results in Fig. 1 show the resonantly enhanced lines at ω_{PM}, $2\omega_{PM}$, $3\omega_{PM}$, and $4\omega_{PM}$. We discuss some of the underlying physical considerations later. Here we emphasize the dramatic enhancement in the intensity of the $\omega_{LO_1}-\omega_{PM}$ line as illustrated in Figs. 4 and 5. The spectra were recorded with the incident polarization along $\hat{z}$, unanalyzed scattered radiation and $\hat{k}_s||\mathbf{H}$. The relatively broad feature at $\sim$220 cm^{-1} is the X_+ luminescence feature attributed to the exciton component at $E_x-3A+3B$. In addition to the LO_1, $LO_1\pm PM$, LO_2, and $LO_2\pm PM$ lines, which have been reported before,[6] two additional features with Raman shifts of $\omega_{LO_1}\pm 2\omega_{PM}$ are observed. A direct consequence of the out-resonance conditions is the pronounced enhancement in the intensity of the LO_1-PM line in Fig. 4 with respect to that of LO_1+PM. In the scattering geometry and the polarization conditions used, the preferential enhancement results from the fact that the polarization of the scattered light for LO_1+ PM is $\hat{\sigma}_-$, while that for LO_1-PM is $\hat{\sigma}_+$, matching that of the X_+ transition. Under nonresonant conditions, for $T=5$ K and $H=60$ kG, the intensity of LO_1+PM would be five times greater than that of LO_1-PM, as calculated from the Boltzmann factor. This enhancement of LO_1-PM becomes even more pronounced under exact out resonance achieved by decreasing the magnetic field to 35 kG and moving the X_+ luminescence feature under the LO_1 and the LO_1-PM Raman lines; this illustrated in Fig. 5 where the LO_1-PM Ra-

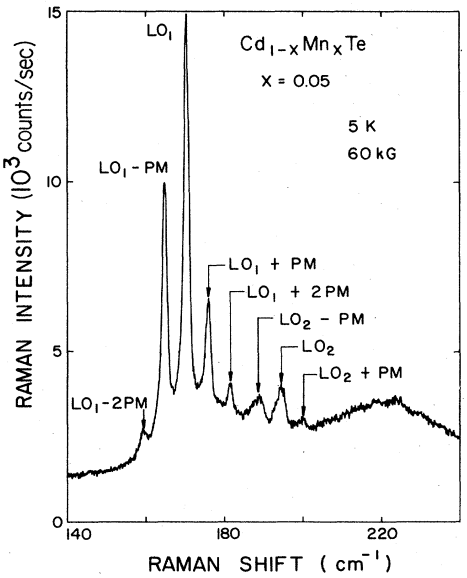

FIG. 4. Raman spectrum of $Cd_{0.95}Mn_{0.05}Te$ in the region of the LO phonons with $T=5$ K, $H=60$ kG, $\lambda_L=7525$ Å, and $P_L=30$ mW. Incident light polarized along $\hat{\mathbf{z}}||\mathbf{H}||\hat{\mathbf{k}}_S$ and scattered light unanalyzed.

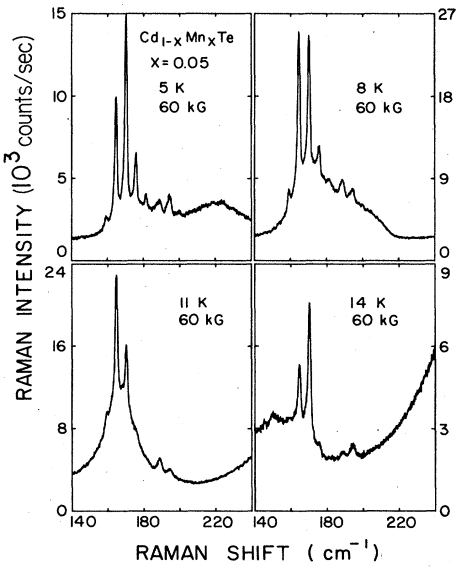

FIG. 6. Temperature variation of the resonance Raman scattering in $Cd_{0.95}Mn_{0.05}Te$ in the region of the LO phonons with $H=60$ kG, and other conditions as in Fig. 4.

man line is more intense than the LO_1 line. The LO_2-PM, LO_2, and LO_2+PM Raman lines show similar effects as can be seen from a comparison of Figs. 4 and 5. In Fig. 6, the resonance conditions are controlled by keeping $H=60$ kG but varying the temperature over the range 4.5–25 K. As can be clearly seen, the resonance enhancement at $T=11$ K and $H=60$ kG is almost identical to that at $T=5$ K and $H=35$ kG. We note that the Raman shift $\omega_{LO}\pm\omega_{PM}$ is insensitive to temperature variation while the position of the Zeeman component of the

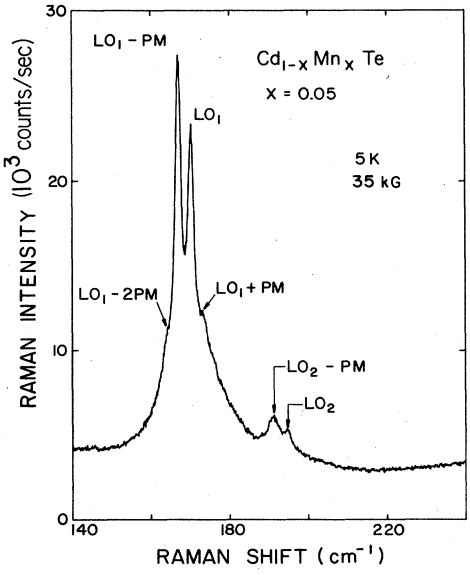

FIG. 5. Raman spectrum of $Cd_{0.95}Mn_{0.05}Te$ in the region of the LO phonons with $H=35$ kG and other conditions as in Fig. 4.

exciton and, hence, the resonance conditions are strongly temperature dependent for the reasons already emphasized.

We now discuss the origin of the Raman lines in Fig. 1 with shifts of $3\omega_{PM}$ and $4\omega_{PM}$, corresponding to $\Delta m_S=3$ and 4, respectively. Multiple spin-flip Raman scattering from electrons bound to donors[19,20] has been reported in the literature and explained invoking either an exchange coupling among donor spins[21] or multiple scattering.[22] The multiple spin-flip features in DMS can be accounted for in terms of excitations within neighboring pairs of Mn^{2+} ions coupled antiferromagnetically and assuming an anisotropic exchange interaction between the ground-state multiplet of one and an excited state of the other; in this model we replace the intermediate step in Eq. (1), i.e., $\langle m_S+1,b\,|\,H_{ex}\,|\,m_S,a\rangle$, with one in which the exchange interaction is now between the electron and a *pair* of neighboring Mn^{2+}. In fact, a pair of neighboring Mn^{2+} in their $^6S_{5/2}$ states in a magnetic field $\mathbf{H}||\hat{\mathbf{z}}$ can be described by the Hamiltonian

$$H=g\mu_B HS_z-J(S^2-\tfrac{35}{2})\,, \tag{4}$$

where J is a Mn^{2+}-Mn^{2+} exchange interaction and $\mathbf{S}=\mathbf{S}^{(1)}+\mathbf{S}^{(2)}$. In a Raman transition, one of the Mn^{2+} ions can experience a virtual excitation to an $L=1$ state. The exchange interaction between a Mn^{2+} ion in its ground state and another in an excited state will, in general, lack rotational invariance. Thus, virtual transitions to intermediate states need not conserve the total (pair + the photon) angular momentum and S_z can change by more than one unit. Such transitions followed by a final transition to one having a value of S *equal* to that of the initial state but having S_z differing by $\Delta S_z=0,\ \pm1,\pm2,\pm3,\ \pm4$, and ±5 yields a Raman shift of $g\mu_B H\Delta S_z$, i.e., a multiple of ω_{PM}, independent of J. Of

course, $S=0$ state is to be excluded as it will not result in a Raman shift; but $S=1$ and higher states are populated because $|J| \sim 2$ K in $Cd_{1-x}Mn_xTe$.[8] In our model the intensities of ω_{PM} and $2\omega_{PM}$ will have contributions from isolated Mn^{2+} as well as Mn^{2+} pairs. The contribution of the latter will have a temperature dependence characteristic of the population of the $S=1$, 2, 3, 4, and 5 multiplets lying 2, 6, 12, 20, and 30 times $|J|$ above the $S=0$ state. The $3\omega_{PM}$ and $4\omega_{PM}$ will have contributions only from $S=2$, 3, 4, and 5 and hence will be correspondingly weaker.

III. CONCLUDING REMARKS

The magnetic field and temperature-tuned resonant Raman scattering discussed in this paper is another example of the unique role played by the strong Mn^{2+}-band-electron exchange interaction in DMS as manifested in the large g factors characterizing the Zeeman splitting of the exciton. It is also of interest to note that the Raman scattering associated with the spin flip of Mn^{2+} (the Raman EPR of Mn^{2+}) is mediated by the creation of an electron-hole pair, or equivalently, an exciton. It is known that $Cd_{1-x}Mn_xTe$ exhibits magnetic ordering at low temperatures[23] and a one-magnon Raman line[8] (the Raman-antiferromagnetic line) which splits into a doublet in an external magnetic field.[6] It has also been demonstrated that as the temperature is lowered and the magnetic order sets in, the Raman-EPR line evolves smoothly into the high-energy component of the one-magnon doublet. This shows that the excitation of an antiferromagnetic spin wave in DMS by inelastic light scattering is also mediated by interband transitions.

ACKNOWLEDGMENTS

The work reported in this paper was supported by National Science Foundation (NSF) Grant Nos. DMR-81-06144 and DMR-84-03325 and benefited from the Central Laser Facility operated under the NSF Materials Reasearch Laboratories Program under Grant No. DMR-83-20249. We thank J. K. Furdyna and U. Debska for providing high-quality samples. One of us (D.L.P.) gratefully acknowledges support by the Eastman Kodak company.

[1] J. K. Furdyna, J. Appl. Phys. **53**, 7637 (1982).
[2] J. A. Gaj, J. Ginter, and R. R. Galazka, Phys. Status Solidi B **89**, 655 (1978).
[3] A. Twardowski, M. Nawrocki, and J. Ginter, Phys. Status Solidi B **96**, 497 (1979).
[4] J. A. Gaj, R. R. Galazka, and M. Nawrocki, Solid State Commun. **25**, 193 (1978).
[5] A. Petrou, D. L. Peterson, S. Venugopalan, R. R. Galazka, A. K. Ramdas, and S. Rodriguez, Phys. Rev. Lett. **48**, 1036 (1982).
[6] A. Petrou, D. L. Peterson, S. Venugopalan, R. R. Galazka, A. K. Ramdas, and S. Rodriguez, Phys. Rev. B **27**, 3471 (1983).
[7] D. L. Peterson, Ph.D. thesis, Purdue University, 1984 (unpublished).
[8] S. Venugopalan, A. Petrou, R. R. Galazka, A. K. Ramdas, and S. Rodriguez, Phys. Rev. B **25**, 2681 (1982).
[9] R. Loudon, Adv. Phys. **13**, 423 (1964).
[10] A. S. Barker, Jr. and R. Loudon, Rev. Mod. Phys. **44**, 18 (1972).
[11] R. Planel, J. Gaj, and C. Benoit a la Guillaume, J. Phys. (Paris) Colloq. **41**, C5-39 (1980); A. Golnik, J. Ginter, and J. A. Gaj, J. Phys. C **16**, 6073 (1983).
[12] K. Zanio, in *Semiconductors and Semimetals, Vol. 13: Cadmium Telluride,* edited by R. K. Willardson and A. C. Beer (Academic, New York, 1978), p. 100.
[13] Y. R. Lee and A. K. Ramdas, Solid State Commun. **51**, 861 (1984).
[14] K. Zanio, in *Semiconductors and Semimetals, Vol. 13: Cadmium Telluride,* Ref. 12, p. 151.
[15] K. Zanio, in *Semiconductors and Semimetals, Vol. 13: Cadmium Telluride,* Ref. 12, p. 139.
[16] K. Zanio, in *Semiconductors and Semimetals, Vol. 13: Cadmium Telluride,* Ref. 12, p. 144.
[17] S. M. Ryabchenko, O. V. Terletskii, I. B. Mizetskaya, and G. S. Oleinik, Fiz. Tekh. Poluprovodn. 15, 2314 (1981) [Sov. Phys.—Semicond. **15**, 1345 (1981)].
[18] We use $(N_0\alpha)=220$ meV and $(N_0\beta)=-880$ meV given by J. A. Gaj, R. Planel, and G. Fishman, Solid State Commun. **29**, 435 (1979).
[19] Y. Oka and M. Cardona, Phys. Rev. B **23**, 4129 (1981); J. Phys. (Paris) Colloq. **42**, C6-459 (1981).
[20] J. F. Scott and T. C. Damen, Phys. Rev. Lett. **29**, 107 (1972); J. F. Scott, T. C. Damen, and P. A. Fleury, Phys. Rev. B **6**, 3856 (1972).
[21] E. N. Economou, J. Ruvalds, and K. L. Ngai, Phys. Rev. Lett. **29**, 110 (1972).
[22] P. A. Wolff, as quoted by S. Geschwind and R. Romestain, in *Light Scattering in Solids IV,* edited by M. Cardona and G. Güntherodt (Springer, Berlin, 1984).
[23] R. R. Galazka, S. Nagata, and P. H. Keesom, Phys. Rev. B **22**, 3344 (1980).